



The performance assessment of nanofluid-based PVTs with and without transparent glass cover: outdoor experimental study with thermodynamics analysis

Amin Taheri¹ · Mohsen Kazemi¹ · Moein Amini¹ · Mohammad Sardarabadi² · Ali Kianifar¹

Received: 12 October 2019 / Accepted: 9 January 2020
© Akadémiai Kiadó, Budapest, Hungary 2020

Abstract

The main objective of current work is to scrutinize the performance of unglazed photovoltaic thermal system (PVTs) and transparent glazed photovoltaic thermal system (GPVTs) from energy and exergy standpoints using four different operating fluids consisting of deionized water, GNP/water, SWCNT/water, and MWCNT/water nanofluids with a mass concentration of 0.05%. Sunny and stable days with the clear sky of September and October are selected as the suitable actual conditions. The outdoor experiments are carried out from 9:30 to 16:00. The results reveal that in the GPVTs, although using a transparent glass cover has an undesirable effect on the surface temperature, electrical output power, and electrical efficiency, the concurrent effect of the glass cover and nanofluid considerably increases the thermal and overall efficiencies. Among all studied operating fluids, the GNP/water and SWCNT/water nanofluids would be more efficient in terms of energy and exergy performances. Regarding the energy viewpoint, the overall efficiencies of GPVTs/MWCNT, GPVTs/SWCNT, and GPVTs/BNP are higher by 12.32%, 17.02%, and 22.65%, respectively, compared to those of PVTs with deionized water. Moreover, from the exergy viewpoint, the overall efficiencies of PVTs/water, PVTs/MWCNT, PVTs/SWCNT, and PVTs/BNP are higher by 1.42%, 1.68%, 1.93%, and 2.32%, respectively, compared to those of the PV unit.

Keywords Energy · Exergy · Transparent glass cover · Photovoltaic thermal system · Solar energy

List of symbols

A	Area/m ²
C_p	Specific heat capacity/J kg ⁻¹ K ⁻¹
\dot{E}	Energy rate/W
\dot{E}_x	Exergy rate/W
FF	Filled factor
\dot{G}	Solar radiation rate/W m ⁻²
I	Electrical current/A
\dot{m}	Mass flow rate/kg s ⁻¹

T	Temperature/K
V	Electrical voltage/V

Greeks symbols

α	Absorptivity of panel
η	Energy efficiency/%
ε	Exergy efficiency/%
ρ	Density/kg m ⁻³
ϕ	Volume concentration
τ	Glass cover transmissivity

Subscripts

Amb	Ambient
Bf	Base fluid
C	Collector
Cell	Photovoltaic cell
Dest	Destruction
El	Electrical
F	Fluid
G	Glass cover
In	Input
N	Nanoparticle
Oc	Open circuit

Amin Taheri and Mohsen Kazemi have equal contribution in this work as the first author.

✉ Mohammad Sardarabadi
m.sardarabadi@yahoo.com

✉ Ali Kianifar
a-kiani@um.ac.ir

¹ Department of Mechanical Engineering, Ferdowsi University of Mashhad, Mashhad, Iran

² Department of Energy, Quchan University of Technology, Quchan, Iran

Outlet	Outlet
Sc	Short circuit
Th	Thermal

Abbreviation

PV	Photovoltaic unit
PVTs	Photovoltaic thermal system
GPVTs	Photovoltaic thermal system with a glass cover

Introduction

The fossil fuel reduction, the swelling population, the environmental pollution, and the change in weather conditions are some of the detrimental problems boosting demand for renewable, clean, and eco-friendly energies. To cope with such drawbacks, solar energy is introduced as one of the best energy sources [1, 2]. Solar thermal collectors and photovoltaic units (PV) are the main solar systems, which can convert solar energy to useful heat and electricity, respectively [3, 4]. Unfortunately, the PV units suffer from the major weakness of decreasing energy efficiency with the increase in surface temperature [5]. To mitigate this problem, photovoltaic thermal systems (PVTs) can extract accumulated heat from PV panels and decrease the surface temperature. In fact, thermal management (TM) of PV panels is considered as a critical issue to enhance power generation [6]. The PVTs are made by attaching a solar thermal collector to PV panels [7]. Although the air [8, 9] and water [10], as operating fluids, are widely used in these hybrid systems, cooling with nanofluids represents an appropriate option owing to the better thermal properties.

Many types of research have been carried out on the performance investigation of PVTs with different nanofluids [11]. From energy and exergy standpoints, Aberoumand et al. [12] studied the performance of PVTs using pure water and Ag/water nanofluid with mass concentrations of 2–4% under various flow regimes. They reported that substituting pure water for the Ag/water nanofluid leads to the enhancement of the power output (8–10%). Al-Waeli et al. [13] compared the thermo-physical properties of CuO, Al₂O₃, and SiC/water nanofluids with volume concentrations of 0.5–4% in the temperature ranged from 25 to 60 °C. Their finding illustrated that the PVTs with SiC/water nanofluid have maximum electrical/thermal efficiencies compared to all conducted studied on operating fluids. The effect of various metal oxides nanoparticles such as Al₂O₃, TiO₂, and ZnO dispersed in pure water with a mass concentration of 0.2% on the PVTs performance was studied by Sardarabadi et al. [14]. They reported that the overall energy and exergy

efficiencies were (47.53%, 11.56%), (57.97%, 11.93%), (59.64%, 12.17%), and (50.1%, 11.88%) for the cases of pure water, TiO₂/water, ZnO/water, and Al₂O₃/water, respectively. Said et al. [15] published a review paper on the performance of conventional and nanofluid-based PVTs and their environmental effects.

In this paragraph, the effects of different types of carbon-based nanofluids on the PVTs performance are deeply investigated. Fayaz et al. [16] numerically and experimentally evaluated the effect of using MWCNT/water nanofluid on the thermal and electrical efficiencies of the PVTs. They observed that the percentage improvement in electrical and thermal performance was achieved by 10.72% and 79.1% in the experimental cases, and 81.24% and 12.25% in the numerical cases by using MWCNT/water. In a similar study, Nasrin et al. [17] assessed the effect of using MWCNT/water nanofluid on the performance of the PVTs. They reported that the enhancement of electrical, thermal, and overall efficiencies of MWCNT/water nanofluid were 0.14%, 3.67%, and 3.81% as they substituted MWCNT/water nanofluid for pure water. Abdallah et al. [18] performed several tests to examine the impact of low concentrations of MWCNT/water nanofluid on the performance of PVTs in the fixed operating flow rate of 1.2 L min⁻¹. It is concluded that the optimum volume concentration of MWCNT/water nanofluid was 0.075%. The effect of using pure water, GNP, SWCNT, and MWCNT/water nanofluids with a mass flow rate of 50 kg/h on the performance of PVTs from energy and exergy standpoints was analyzed by Alshaheen et al. [19]. They found that in the PVTs, using SWCNT, GNP, and MWCNT/water nanofluid instead of PVTs/water, improves the overall energy efficiency by 15.24%, 19.3%, and 9.46%, respectively. In a recent experimental study, from energy and exergy viewpoints, Alous et al. [20] investigated the effect of two different carbon-based nanofluids including MWCNT/water and GNP/water on the performance of PVTs without glass cover. Based on their results, the overall energy efficiency was increased by 53.4% for PVTs/water, 57.2% for PVTs/MWCNT, and 63.1% for GNP/water.

To enhance the thermal and overall energy efficiencies, another applicable and straightforward technique is employing glass cover on the surface of PVTs thanks to greenhouse effects. Based on this phenomenon, the solar thermal energy received is trapped between the glass cover and PVTs surface. On the other hand, the glass cover can be considered a role as an atmosphere. Some investigations performed the thermodynamic analysis to contrast the glazed PVTs with unglazed ones. Yazdanifard et al. [21] mathematically analyzed the effects of various operating parameters on the performance of the PVTs and GPVTs under two flow

regimes. They found that increasing the packing factor and solar irradiation has a positive impact on total energy and exergy efficiencies. Moreover, increasing collector length has a positive effect on total exergy efficiency although the negative effect was found on overall energy efficiency. Chow et al. [22] examined the PVTs and GPVTs from energy and exergy standpoints in a mathematical and experimental study. The effects of operating parameters such as solar irradiation, wind speed, ambient temperature, packing factor, and cell efficiency are evaluated. They concluded that adding a glass cover has positive effects on energy PVTs performance while it leads to adverse effects on exergy performance. Kazemian et al. [23] did experimental research on the performance of PVTs and GPVTs using different operating fluids. Their results indicated that the average thermal energy efficiencies were calculated to be (63.37%, 70.89%) and (44.68%, 53.75%) for the unglazed and glazed cases of PVTs/water and PVTs/pure ethylene glycol, respectively. The corresponding values for electrical efficiencies were equal to (14.35%, 13.15%) and (13.61%, 10.22%), respectively.

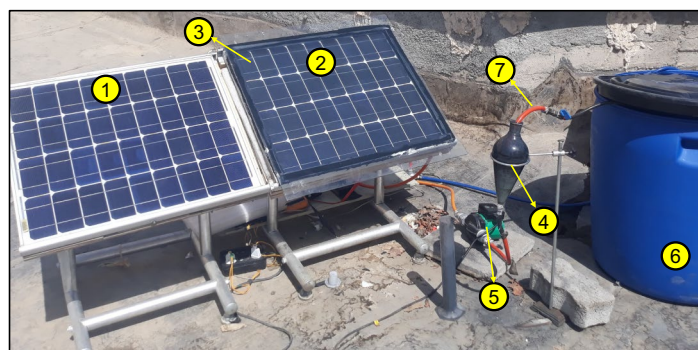
According to the literature review above, nanofluids have inevitable effects on the performance of PVTs, and among all nanofluids, the carbon-based one has been less investigated by researchers. Besides, the attachment of a glass cover layer on the surface of PVTs, owing to increasing greenhouse effects, leads to enhanced surface temperature and thermal efficiency. Rarely, efforts have been made to analyze the effects of the simultaneous use of nanofluid and glass cover on the performance of PVTs. In this research, thus, the performances of PVTs and transparent glazed PVTs are investigated from the energy and exergy point of views. Experiments are run using different nanofluids (GNP/water, SWCNT/water, and MWCNT/water with a mass concentration of 0.05%) with a volume flow rate of 50 kg/h. The working conditions of sunny and stable days of September and October from 9:30 to 16:00 are selected as suitable weather conditions.

The description of the experimental setup and measurement equipment

In this study, two exact similar PV modules with the maximum output electrical power and size of 40 W and (630 mm × 540 mm × 24 mm), respectively, are provided (Fig. 1).

- The first system is a PV unit (Suntech Co., China) without implementing any cooling module. Details of the aforementioned system are reported in Table 1.
- The second system (PVTs) is made with the aid of attaching a copper thermal collector with a serpentine shape to the PV unit (see Fig. 2). Moreover, in order to enhance the heat transfer and decrease thermal resistance, air gaps between the collector and PV unit are filled by thermal interface material (TIM). The inner and outer diameters of the collector are 10 mm and 12 mm, respectively. The copper absorber has a size of 630 mm × 540 mm × 0.4 mm whose details are summarized in Table 1. An AC centrifugal pump is employed to circulate the operating fluid inside the thermal collector, and inlet and outlet operating fluid temperatures are measured via two calibrated PT-100 thermocouples linked to a digital indicator (see Fig. 3).
- The third system (GPVTs) is assembled similar to the second system except its surface is covered via transparent glass cover with the aim of providing the greenhouse effect and increasing thermal efficiency. The glass cover is transparent whose size is 630 mm × 540 mm × 3.2 mm. In addition, the other characteristics are presented in Table 1. The output electrical power of the PV unit, PVTs, and GPVTs is measured using a digital multimeter (UT71C/D/E). Furthermore, the solar irradiation during the experiments is measured by a solar meter (Pyranometer-TES133). Note that the flow rate of 50 kg/h is selected for the operating fluid measured using a timer and measuring vessel. A summary of measurement equipment and accessories utilized in this study is reported in Table 2.

Fig. 1 The image of the experimental rig



- 1: PV unit
- 2: Glazed PVT system
- 3: Transparent glass cover
- 4: Working fluid container
- 5: Circulation pump
- 6: Tank (heat exchanger)
- 7: From heat exchanger

Table 1 Details and dimensions of the PV unit, thermal collector, and transparent glass cover

PV unit	
Type (maximum output power)	Mono-crystalline (40 W)
Fill factor under standard conditions	0.72
Dimensions/mm × mm × mm	630 × 540 × 24
Cell and module efficiency/ %	16 and 15
Brand	Suntech Co.
Cell dimensions/mm × mm	62.5 × 12
Open-circuit voltage/V	21.6
Short-circuit current/A	2.57
Thermal copper collector	
Type	Serpentine
Inner and outer diameter of tubes/mm	10 and 12
Dimensions of absorber plate/mm × mm × mm	630 × 540 × 0.4
Dimensions of insulation layer/mm × mm × mm	630 × 540 × 19
Type of insulation layer	Polyurethane
Glass cover	
Type	Transparent
Dimensions/mm × mm × mm	630 × 540 × 3.2

PV module, GPVTs, and unglazed PVTs with four different cooling fluids (deionized water, GNP, SWCNT, and MWCNT/water nanofluids) are assessed in the current experimental study. The PV, PVTs, and GPVTs are fixed at 30° (tilt angle). All studied nanofluids (GNP, SWCNT, and MWCNT/water) with a mass concentration of 0.05% are

provided from VCN Materials Company, and the characteristics of nanoparticles are reported in Table 3.

Thermodynamic analysis and parameters utilized in calculations

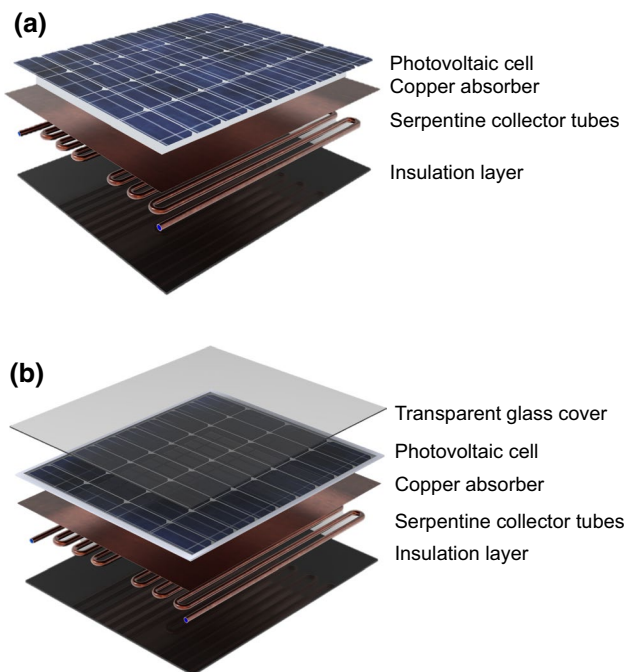
In order to analyze the performance of PVTs and GPVTs in terms of energy and exergy, the PV module and attached serpentine thermal copper collector should be considered as a control volume with the assumption of a semi-steady state condition. Figure 4 depicts the schematic illustration of the energy and exergy balance of PVTs and GPVTs. In addition, regarding the previous study [23], a summary of energy and exergy equations that are used to evaluate the performance of GPVTs is reported in Table 4. It should be noted that the pump power consumption has negligible effects on electrical efficiency reduction [14].

The heat capacity and density of nanofluids can be considered regarding the base fluid and nanoparticle properties (Table 3) and calculated via the next equations [25]:

$$C_{p,nf} = \frac{\phi \cdot (\rho_n \cdot C_{p,n}) + (1 - \phi) \cdot (\rho_{bf} \cdot C_{p,bf})}{\rho_{nf}} \quad (12)$$

$$\rho_{nf} = \phi \cdot \rho_n + (1 - \phi) \cdot \rho_{bf} \quad (13)$$

in which, the subscripts of *bf*, *n*, and *nf* represent base fluid, nanoparticles, and nanofluid, respectively. In addition, ϕ is the volumetric concentration of nanoparticles in the deionized water calculated by the following equation [26]:

**Fig. 2** The exploded view of **a** PVTs and **b** GPVTs

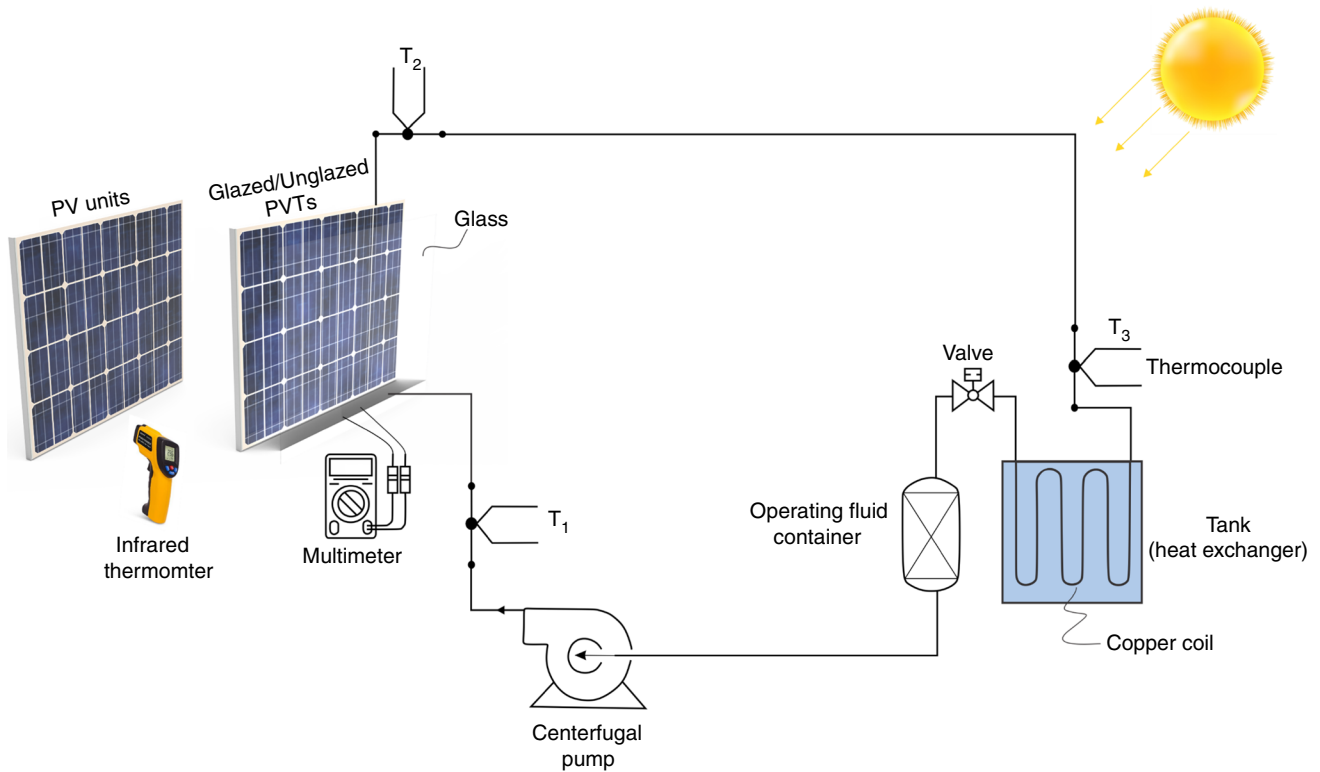


Fig. 3 The schematic illustration of the experimental setup

Table 2 The utilized measurement equipment and accessories in this study

Role	Equipment
Surface temperature	Infrared thermometer
Solar irradiation	Pyranometer (TES133)
Open-circuit voltage and short-circuit current	Digital multi-meter (UT71C/D/E)
Temperatures at inlet and outlet of collector	PT-100 thermocouple
Ambient temperature	Mercury thermometer
Circulation of operating fluid	Inline AC pump

Table 3 Properties of the studied nanoparticles

Nanoparticles	GNP [20]	SWCNT [24]	MWCNT [16, 17]
Heat capacity/kJ kg ⁻¹ K ⁻¹	0.710	0.600	0.796
Thermal conductivity/W m ⁻¹ K ⁻¹	5000	3500	3000
Density/kg m ⁻³	2100	2100	1600

$$\phi = \frac{m_n / \rho_n}{m_n / \rho_n + m_f / \rho_f} \quad (14)$$

in which, m_n and m_f are the mass of nanoparticles and the base fluid, respectively.

Propagation of errors and uncertainty analysis

Based on the propagation of errors, the uncertainty analysis is performed to investigate the reliability of experimental data. More details about the utilized relations used to scrutinize the uncertainties (equipment uncertainty and total uncertainty) of the systems are reported in previous studies

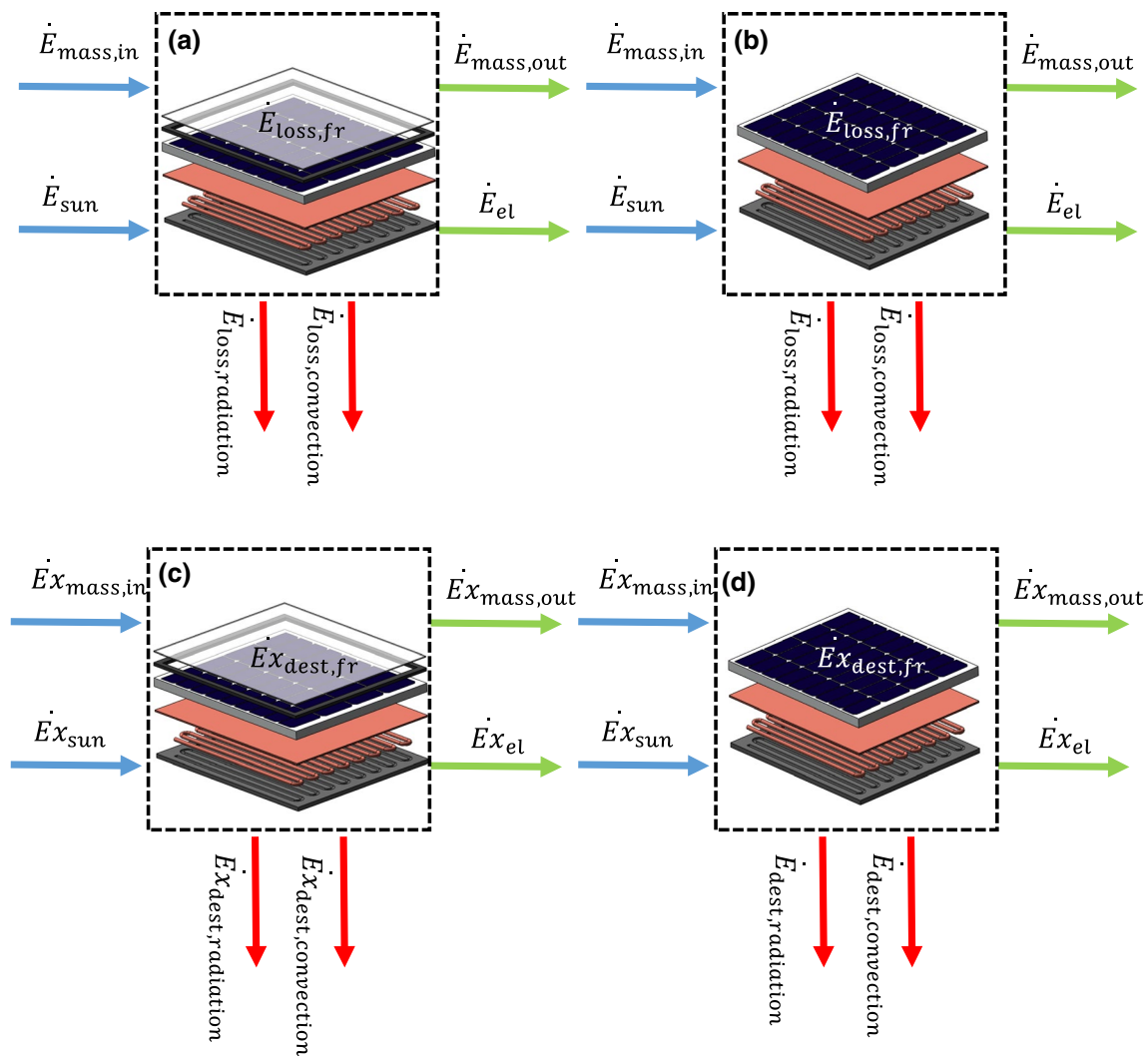


Fig. 4 The schematic illustration of PVTs and GPVTs: **a–b** energy balance and **c–d** exergy balance

[27, 28]. The maximum uncertainties of the experimental setup are shown in Table 5.

Results and discussion

Operating conditions and surface temperature of studied systems

In this experimental research, the effects of deionized water, GNP/water, SWCNT/water, and MWCNT/water nanofluids with a mass concentration of 0.05%, as the operating fluids, are studied on the performance of transparent glazed and unglazed PVTs from both thermodynamic viewpoints (energy and exergy). Outdoor tests are performed on stable days with the clear sky of September and October. It is worth noting that all measured parameters are obtained every 30 min. Figure 5a depicts that the solar irradiation

and temperature of the surrounding during a certain period (from 9:30 to 16:00) in Mashhad. The minimum, maximum, and average of surrounding temperatures are measured to be 27 °C, 33 °C, and 30.85 °C. Additionally, the corresponding values for solar irradiations are 521 Wm⁻², 1032 Wm⁻², and 865 Wm⁻², respectively. Regarding Eq. (4), the sun exergy is calculated and presented in Fig. 5b, in which the minimum and maximum values are achieved at 16:00 and 13:00, respectively. As shown in Fig. 5a, b, the solar irradiation and sun exergy increase from 9:30 to 13:00 followed by a gradual drop.

Figure 6a plots the surface temperature of the unglazed PV unit and PVTs with deionized water, GNP/water, SWCNT/water, and MWCNT/water nanofluids versus local time. Similarly, the changes in the surface temperature of the unglazed PV unit and GPVTs with different operating fluids versus local time are illustrated in Fig. 6b. At first glance, it is observed that the surface temperature of the PV unit is

Table 4 A summary of energy and exergy equations and their details [23]

Eq.	Eq. number	Expression	Details
1st law of thermodynamics	(1)	$\dot{E}_{\text{sun}} + \dot{E}_{\text{mass, in}} = \dot{E}_{\text{lost}} + \dot{E}_{\text{el}} + \dot{E}_{\text{mass, out}}$	–
2nd law of thermodynamics	(2)	$\dot{E}x_{\text{mass, in}} + \dot{E}x_{\text{sun}} = \dot{E}x_{\text{el}} + \dot{E}x_{\text{mass, out}} + \dot{E}x_{\text{dest}}$	–
Sun energy	(3)	$\dot{E}_{\text{sun}} = A \cdot \tau_g \cdot \alpha_{\text{cell}} \cdot \dot{G}$	Herein \dot{G} , A , α_{cell} , and τ_g are solar irradiation, PV surface area, cell absorptivity, and cover transmissivity, respectively.
Sun exergy	(4)	$\dot{E}x_{\text{sun}} = \dot{G}A \left(1 - \frac{T_{\text{amb}}}{T_{\text{sun}}}\right)$	Herein T_{amb} and T_{sun} refer to ambient and sun temperatures, respectively. ($T_{\text{sun}} \cong 5700 \text{ K}$)
Rate of thermal energy	(5)	$\dot{E}_{\text{th}} = \dot{m}_f C_{p,f} (T_{f, \text{out}} - T_{f, \text{in}})$	Herein \dot{m} and $C_{p,f}$ are fluid rate and heat capacity of the operating fluid.
Rate of thermal exergy	(6)	$\dot{E}x_{\text{th}} = \dot{m}_f C_{p,f} \left[(T_{f, \text{out}} - T_{f, \text{in}}) - T_{\text{amb}} \ln \left(\frac{T_{f, \text{out}}}{T_{f, \text{in}}} \right) \right]$	–
Rate of electrical energy and exergy	(7)	$\dot{E}_{\text{el}} = V_{\text{oc}} \cdot I_{\text{sc}} \cdot \text{FF}$	Herein FF, V_{oc} , and I_{sc} are Filled factor, open-circuit voltage, and short-circuit current, respectively.
Thermal energy efficiency	(8)	$\eta_{\text{th}} = \frac{\dot{m}_f C_{p,f} (T_{f, \text{out}} - T_{f, \text{in}})}{A \cdot \tau_g \cdot \alpha_{\text{cell}} \cdot \dot{G}}$	–
Thermal exergy efficiency	(9)	$\epsilon_{\text{th}} = \frac{\dot{m}_f C_{p,f} \left[(T_{f, \text{out}} - T_{f, \text{in}}) - T_{\text{amb}} \ln \left(\frac{T_{f, \text{out}}}{T_{f, \text{in}}} \right) \right]}{\dot{E}x_{\text{sun}}}$	–
Electrical energy efficiency	(10)	$\eta_{\text{el}} = \frac{\dot{E}_{\text{el}}}{\dot{E}_{\text{sun}}} = \frac{I_{\text{sc}} \times V_{\text{oc}} \times \text{FF}}{A \cdot \tau_g \cdot \alpha_{\text{cell}} \cdot \dot{G}}$	–
Electrical exergy efficiency	(11)	$\epsilon_{\text{el}} = \frac{\dot{E}_{\text{el}}}{\dot{E}_{\text{sun}}} = \frac{I_{\text{sc}} \times V_{\text{oc}} \times \text{FF}}{\dot{E}x_{\text{sun}}}$	–

Table 5 The accuracy of the instrument and the maximum uncertainty of experimental data

Instrument (model)	Measurement section	Accuracy	Maximum uncertainty
Solar meter (TES-133)	Solar irradiation	$\pm 10 \text{ W m}^{-2} + 0.38 \text{ W m}^{-2}$ for ($T_{\text{ref}} + 1$)	6.1 W m^{-2}
Multi-meter (UT71C/D/E)	Open-circuit voltage	$\pm (0.5\% + 1)$	0.08 V
Multi-meter (UT71C/D/E)	Short-circuit current	$\pm (0.5\% + 1)$	0.03 A
Thermometer (Infrared K)	Surface temperature	$\pm 0.25 \text{ }^\circ\text{C}$	0.19 $^\circ\text{C}$
Thermocouple (RTD/PT100)	Operating fluid temperature	$\pm 0.15 \text{ }^\circ\text{C}$ to $\pm 0.25 \text{ }^\circ\text{C}$	0.17 $^\circ\text{C}$
Thermometer (Mercury)	Ambient temperature	$\pm 0.5 \text{ }^\circ\text{C}$	0.2 $^\circ\text{C}$

decreased, as a result of attaching a thermal collector as a cooling module. Secondly, the average surface temperatures of unglazed cases of PV unit, PVTs/water, PVTs/MWCNT, PVTs/SWCNT, and PVTs/GNP are 59.69 $^\circ\text{C}$, 38.22 $^\circ\text{C}$, 35.80 $^\circ\text{C}$, 34.26 $^\circ\text{C}$, and 33.32 $^\circ\text{C}$, respectively. The PVTs with nanofluids experience a lower average surface temperature due to higher thermal conductivity. However, according to Fig. 6b, the GPVTs in all studied period test have higher surface temperature owing to greenhouse effect between the PVTs surface and glass cover. Figure 6b presents that, compared to unglazed PVTs, the GPVTs cases have greater average surface temperature by 6.12 $^\circ\text{C}$, 6.15 $^\circ\text{C}$, 6.11 $^\circ\text{C}$, and 5.58 $^\circ\text{C}$ in the cases of GPVTs/water, GPVTs/MWCNT,

GPVTs/SWCNT, and GPVTs/GNP, respectively. According to Fig. 6a, b, the variation of surface temperature has the same trend compared to that of variation solar irradiation. Furthermore, the increase in solar irradiation leads to the rise of the surface temperature.

Electrical analysis from energy and exergy viewpoints

Figure 7a, b shows the variation of daily electrical power production of the unglazed PVTs and GPVTs, respectively. Firstly, it is observed that the electrical power profile of all systems follows the same trend of the figure of solar

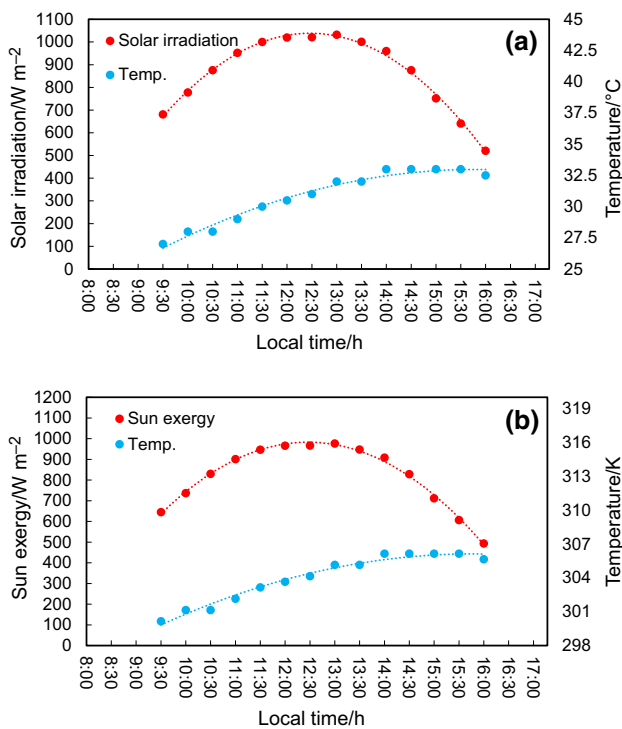


Fig. 5 Change in ambient temperature, **a** solar irradiation, and **b** sun exergy versus local time

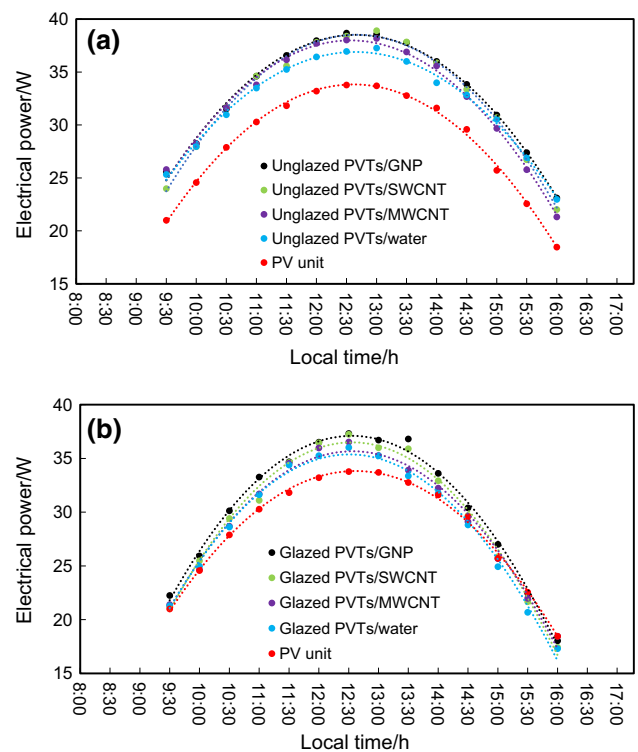


Fig. 7 The change in output electrical power of the unglazed PV unit and **a** unglazed PVTs and **b** GPVTs versus local time

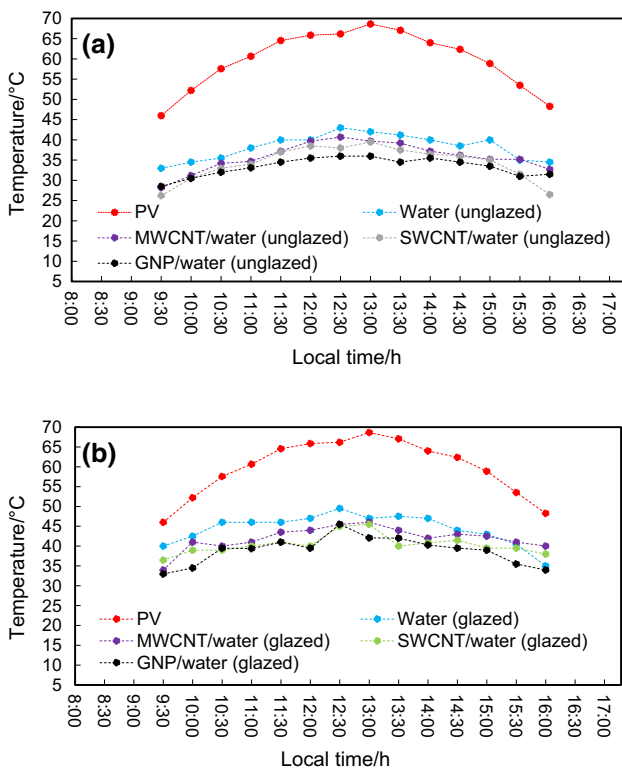


Fig. 6 Change in surface temperature of the unglazed PV unit and **a** unglazed PVTs, and **b** GPVTs versus local time

irradiation. It is found that the maximum and minimum values of electrical power are obtained in the noon and afternoon, respectively. Secondly, comparing the electrical power trends of Fig. 7a, b during the day reveals that in the same operating fluid, the unglazed PVTs produce higher electrical output owing to lower surface temperature (see Fig. 6). In addition, in both PVTs and GPVTs, the GNP/water seems to have a higher potential to increase electrical power compared to other operating fluids. The average electrical power of unglazed PV, PVTs/water, PVTs/MWCNT, PVTs/SWCNT, and PVTs/GNP is measured to be 28.34 W, 31.91 W, 32.24 W, 32.52 W, and 32.90 W, respectively. These values for unglazed PV, GPVTs/water, GPVTs/MWCNT, GPVTs/SWCNT, and GPVTs/GNP are 28.34 W, 28.87 W, 29.29 W, 29.63 W, and 30.36 W, respectively. This can be comprehended that, regrettably, because of reduced heat rejection between surface and glass cover, using a glass cover has an inverse effect on the performance of GPVTs from the electrical viewpoint.

With the aid of Eqs. (10) and (11), the average electrical energy and exergy efficiencies of all cases are depicted in Fig. 8a, b, respectively. It is clear that similar to Fig. 7, due to better thermal properties and heat transfer mechanisms, the GNP/water nanofluid has considerable impacts on the performance of PVTs in both PVTs and transparent GPVTs. In this way, as the values of electrical power decrease in

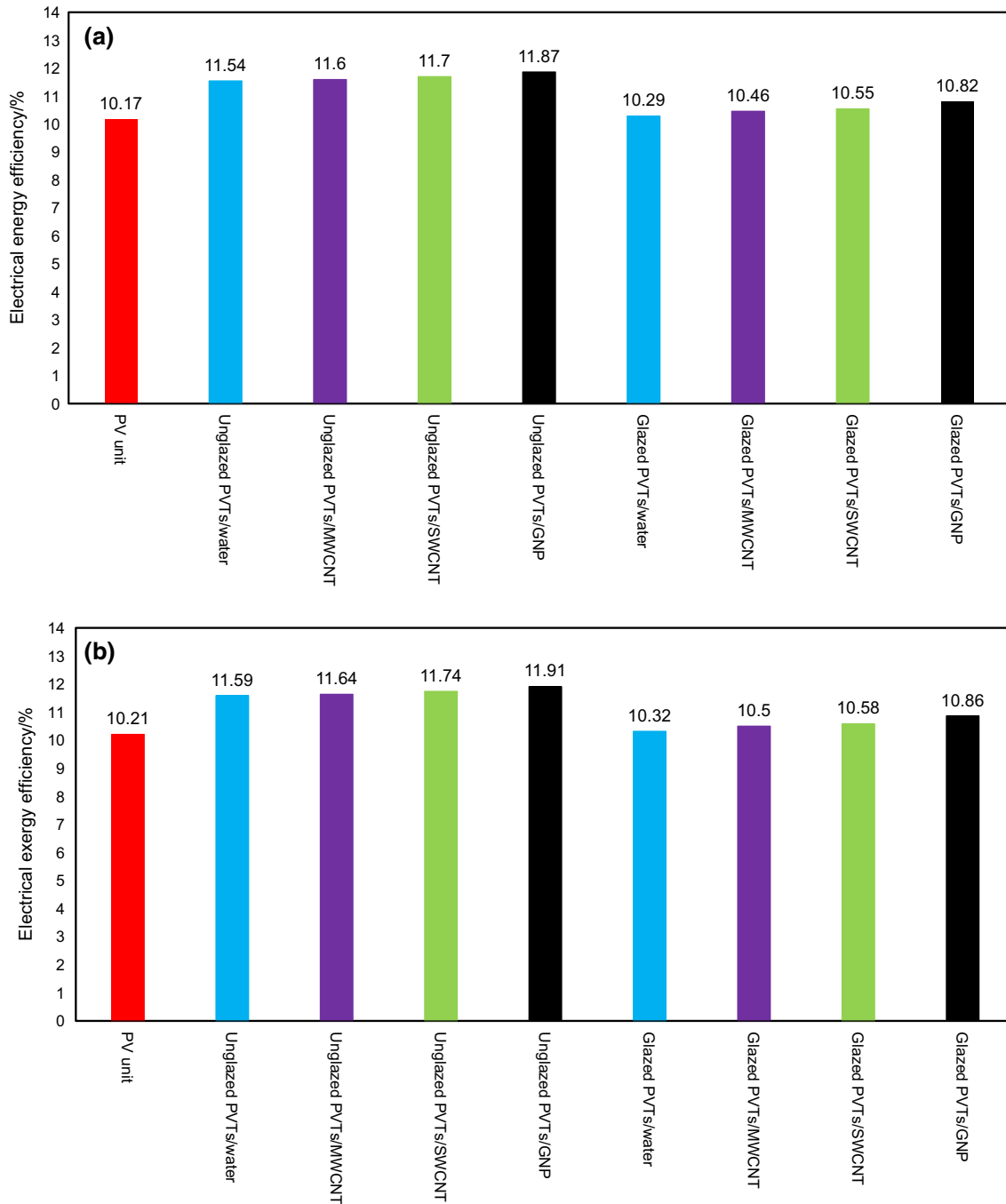


Fig. 8 Average electrical efficiency of the PV unit, PVTs, and GPVTs from **a** energy viewpoint and **b** exergy viewpoint

GPVTs, the value of electrical efficiencies (both thermodynamic viewpoints) decreases as expected.

Although based on Fig. 7, the value of electrical energy is equal to that of electrical exergy, in the same system/operating fluid, the values of exergy efficiency are higher than those of energy efficiency. Based on Eqs. (3) and (4), the

values of available solar energy are higher than those of solar exergy. It is observed from Fig. 8a that the unglazed PVTs with the GNP/water, SWCNT/water, MWCNT/water, and deionized water have as great as energy efficiency by 1.7%, 1.54%, 1.43%, and 1.37%, respectively, in comparison

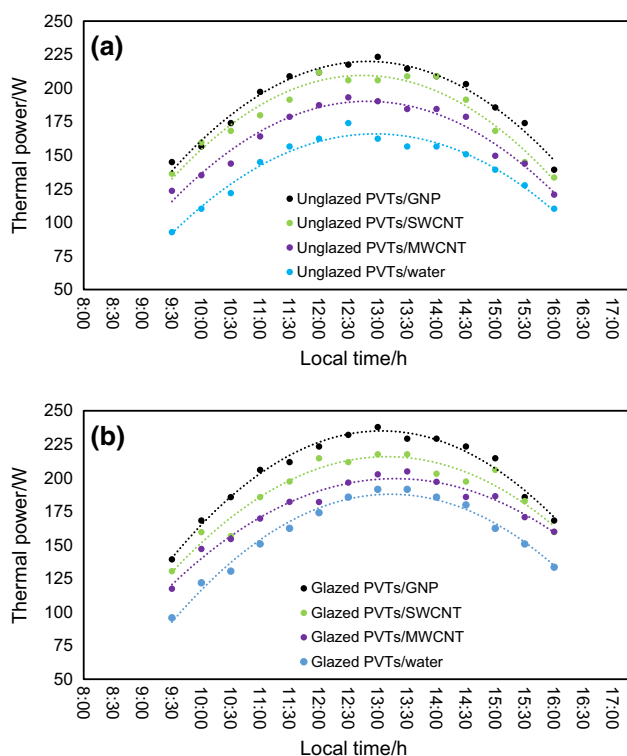


Fig. 9 The variation of thermal energy of **a** unglazed PVTs and **b** GPVTs versus local time

with the energy efficiencies of the PV unit. These values for GPVTs are 0.56%, 0.38%, 0.29%, and 0.12%, respectively.

Thermal energy and exergy analysis

In this sub-section, by using Eqs. (5) and (6), the effect of simultaneous use of various operating fluids and glass cover is studied on the performance of PVTs from thermal energy and exergy viewpoints. Figure 9a, b represents that the variation of thermal energy of unglazed PVTs and GPVTs is a function of local time/solar irradiation. Additionally, the average thermal exergy of both systems, with different cooling fluids, is illustrated in Fig. 10. The results indicate that the thermal exergy of GPVTs is more than those of PVTs, which is due to the growth of surface temperature and the reduction in the heat losses from the PVTs. Consequently, using the glass cover can be considered as a positive factor. Besides, Figs. 9 and 10 prove that higher thermal conductivity of nanofluids leads to the enhancement of the thermal energy and exergy in PVTs and GPVTs compared to those systems that use deionized water. The average thermal energy of PVTs is 190.4 W, 179.68 W, 162.77 W, and 140.51 W with GNP/water, SWCNT/water, MWCNT/water, and deionized water, respectively, and these values for the GPVTs are calculated to be 203.93 W, 188.59 W, 177.51 W,

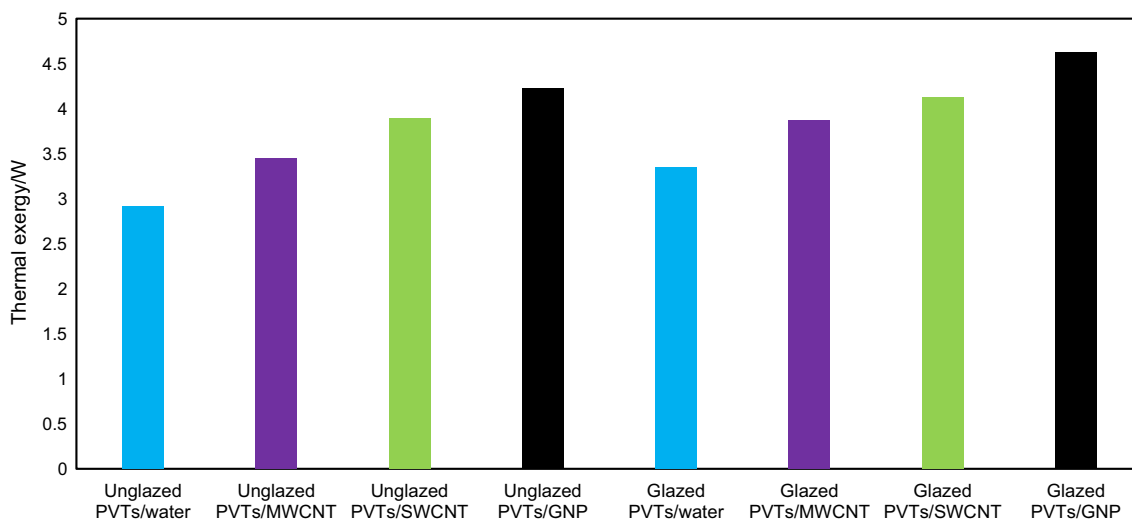


Fig. 10 Average thermal exergy of PVTs and GPVTs

Table 6 Average thermal energy and exergy efficiencies of glazed and unglazed PVTs

System (operating fluid)	PVTs GNP	GPVTs GNP	PVTs SWCNT	GPVTs SWCNT	PVTs MWCNT	GPVTs MWCNT	PVTs water	GPVTs water
Thermal energy efficiency/ %	68.87	74.23	64.93	68.87	58.88	64.29	50.86	57.53
Thermal exergy efficiency/ %	1.53	1.68	1.4	1.50	1.25	1.41	1.05	1.21

and 158.83 W, respectively. The values of thermal exergy for the GPVTs/GNP, GPVTs/SWCNT, GPVTs/MWCNT, and GPVTs/water are improved by roughly 0.4 W, 0.23 W, 0.42 W, and 0.44 W, respectively, compared to those of the PVTs/GNP, PVTs/SWCNT, PVTs/MWCNT, and PVTs/water.

The average thermal energy and exergy efficiencies of both PVTs and GPVTs using different operating fluids are reported in Table 6. As it is mentioned earlier, adding nanoparticles to the base fluid and using a glass cover on PVTs can improve both thermal energy and exergy efficiencies. The thermal energy and exergy efficiencies of GPVTs/GNP increased by 23.37% and 0.63%, respectively, compared with the efficiencies of PVTs/water. Based on this table, the use of GNP/water and SWCNT/water nanofluids, because of their higher thermal properties such as thermal conductivity, would be more efficient in terms of thermal/overall energy and exergy.

The analysis of overall energy and exergy

To elucidate, the average electrical and thermal efficiencies are indicated for PV unit, PVTs/water, and GPVTs/GNP (Fig. 11a–c). Although the electrical efficiency of GPVTs is slightly lower than that of PVTs, the thermal and overall efficiencies of GPVTs with GNP/water nanofluid are higher by 23.37% and 22.65%, respectively, compared to those of PVTs/water. Thus, the thermal and overall efficiencies of PVTs are greatly influenced by operating fluid (nanofluid) and using glass cover, in turn, increases the thermal and overall efficiencies.

Figure 12a–b reports a summary of efficiencies (electrical and thermal) of PV, PVTs, and GPVTs using various coolants from energy and exergy standpoints, respectively. According to these figures, some key points can be deduced. Firstly, although the glass cover has an unfavorable effect on PVTs electrical efficiency, it can be concluded that the use of nanofluids and glass cover has a favorable effect on PVTs in terms of thermal and overall efficiencies. Secondly, based on Fig. 12b, due to the more contribution of electrical exergy efficiency in the overall exergy efficiency, using a glass cover has an inverse effect from an exergy viewpoint. It is observed that the overall energy efficiencies of GPVTs/MWCNT, GPVTs/SWCNT, and GPVTs/GNP are higher by 12.32%, 17.02%, and 22.65%, respectively, compared to those of PVTs/water. Additionally, the overall exergy efficiencies of PVTs/water, PVTs/MWCNT, PVTs/SWCNT, and PVTs/GNP are higher by 1.42%, 1.68%, 1.93%, and 2.32%, respectively, compared to those of PV unit. The results of the present study can be compared with Ref. [20], in which the authors used water, GNP/water, and MWCNT/water as the coolants in PVTs without glass cover. Their results showed that the total energy efficiency of PVTs/water, PVTs/MWCNT, and PVTs/GNP was improved by 53.4%, 57.2%, and 63.1%, respectively. Therefore, in both studies, the use of GNP/water has a better performance compared to that of deionized water and MWCNT/water.

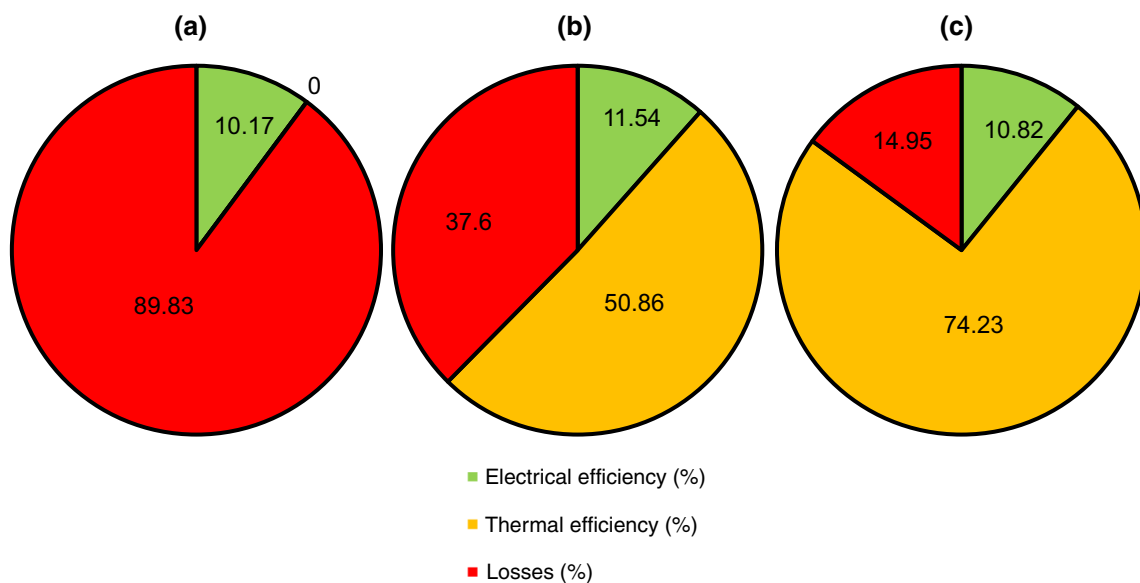


Fig. 11 The contribution of electrical and thermal efficiencies of a PV unit, b PVTs/water, and c GPVTs/GNP

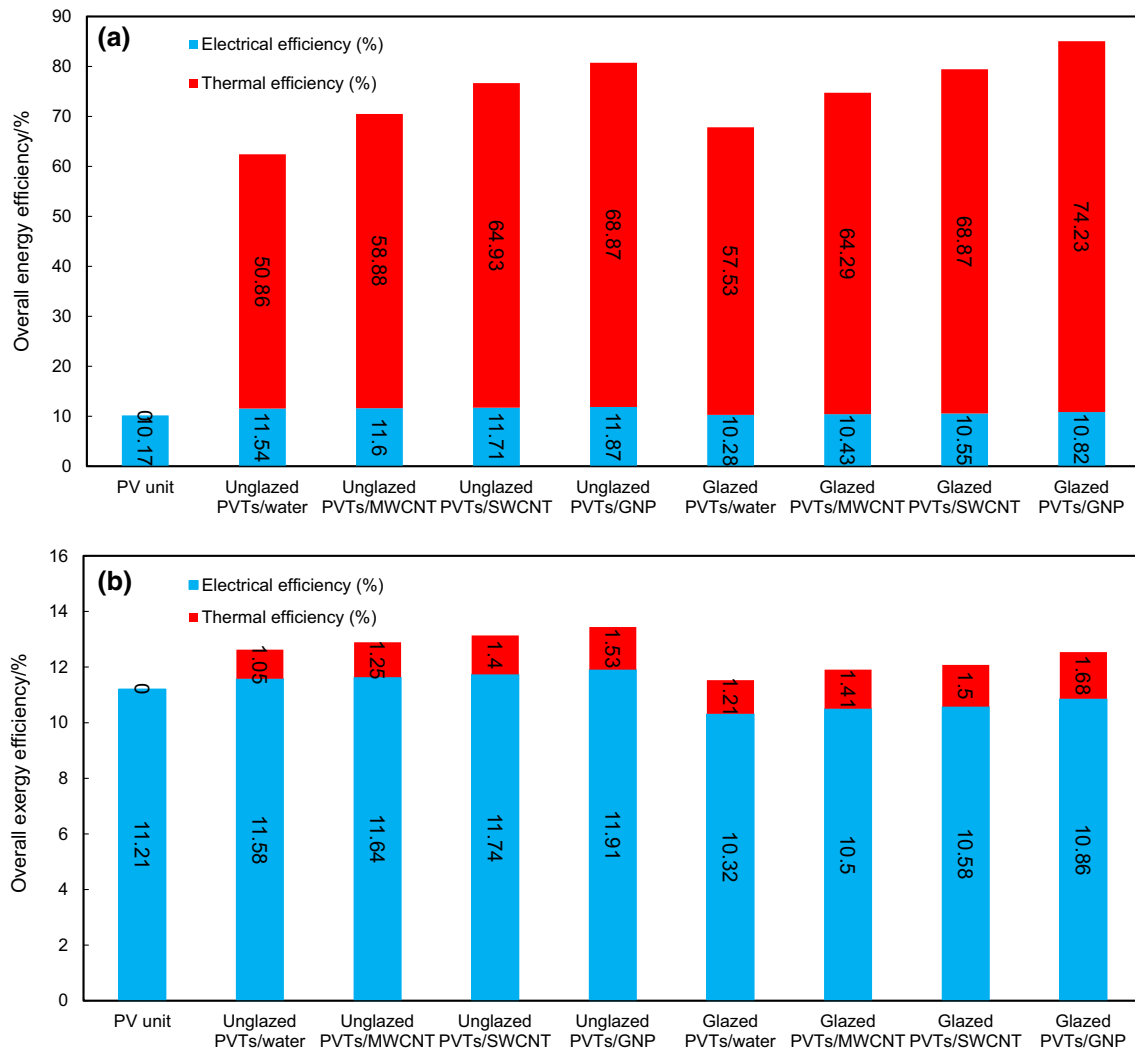


Fig. 12 Average overall efficiencies of PVTs and GPVTs from viewpoints of **a** energy and **b** exergy

Conclusions

In this paper, the performance of PVTs and GPVTs using deionized water and three various nanofluids (GNP/water, SWCNT/water, and MWCNT/water) was studied under actual outdoor conditions in sunny days with a clear sky, and the results were analyzed from the energy and exergy points of views. The main findings are enumerated as follows:

1. In GPVTs, although using a glass cover causes consequences on the surface temperature, the electrical energy, the electrical exergy, and the electrical efficiencies, the thermal and overall efficiencies considerably increase.
2. Among all studied operating fluids, the GNP/water and SWCNT/water thanks to their thermal properties improve the electrical, the thermal, and the overall energy/exergy efficiencies.
3. The average thermal energy of PVTs was measured to be 190.4 W, 179.68 W, 162.77 W, and 140.51 W with GNP/water, SWCNT/water, MWCNT/water nanofluids, and deionized water, respectively, and the corresponding values for GPVTs are 203.93 W, 188.59 W, 177.51 W, and 158.83 W, respectively.
4. The thermal exergy of the GPVTs/GNP, GPVTs/SWCNT, GPVTs/MWCNT, and GPVTs/water was improved by virtually 0.4 W, 0.23 W, 0.42 W, and 0.44 W, respectively, in comparison with that of the PVTs/GNP, PVTs/SWCNT, PVTs/MWCNT, and PVTs/water.
5. The overall energy efficiency of GPVTs/MWCNT, GPVTs/SWCNT, and GPVTs/GNP was improved by 12.32%, 17.02%, and 22.65%, respectively, compared to that of PVTs with deionized water.
6. Compared to the overall exergy efficiency of PV unit, that of PVTs/water, PVTs/MWCNT, GPVTs/SWCNT,

and GPVTs/GNP was as great as by 1.42%, 1.68%, 1.93, and 2.32%, respectively.

References

1. Amini M, Kianifar A, Edalatpour M, editors. An analytical study on energy and exergy of a minichannel-based solar collector using Fe₃O₄ and MgO/water nanofluids. In: International conference on researches in science and engineering; 2016.
2. Ammar AA, Sopian K, Alghoul MA, Elhub B, Elbreki AM. Performance study on photovoltaic/thermal solar-assisted heat pump system. *J Therm Anal Calorim*. 2019;136(1):79–87. <https://doi.org/10.1007/s10973-018-7741-6>.
3. Kazemian A, Salari A, Hakkaki-Fard A, Ma T. Numerical investigation and parametric analysis of a photovoltaic thermal system integrated with phase change material. *Appl Energy*. 2019;238:734–46. <https://doi.org/10.1016/j.apenergy.2019.01.103>.
4. Gangadevi R, Vinayagam BK. Experimental determination of thermal conductivity and viscosity of different nanofluids and its effect on a hybrid solar collector. *J Therm Anal Chem*. 2019;136(1):199–209. <https://doi.org/10.1007/s10973-018-7840-4>.
5. Hossain MS, Pandey AK, Selvaraj J, Abd Rahim N, Rivai A, Tyagi VV. Thermal performance analysis of parallel serpentine flow based photovoltaic/thermal (PV/T) system under composite climate of Malaysia. *Appl Therm Eng*. 2019. <https://doi.org/10.1016/j.applthermaleng.2019.01.007>.
6. Khanna S, Newar S, Sharma V, Reddy KS, Mallick TK, Radulovic J, et al. Electrical enhancement of solar photovoltaic using phase change material. *J Clean Prod*. 2019. <https://doi.org/10.1016/j.jclepro.2019.02.169>.
7. AL-Musawi AIA, Taheri A, Farzanehnia A, Sardarabadi M, Passandideh-Fard M. Numerical study of the effects of nanofluids and phase-change materials in photovoltaic thermal (PVT) systems. *J Therm Anal Calorim*. 2019;137(2):623–36. <https://doi.org/10.1007/s10973-018-7972-6>.
8. Fudholi A, Zohri M, Rukman NSB, Nazri NS, Mustapha M, Yen CH, et al. Exergy and sustainability index of photovoltaic thermal (PVT) air collector: a theoretical and experimental study. *Renew Sustain Energy Rev*. 2019;100:44–51. <https://doi.org/10.1016/j.rser.2018.10.019>.
9. Kumar R, Rosen MA. A critical review of photovoltaic–thermal solar collectors for air heating. *Appl Energy*. 2011;88(11):3603–14. <https://doi.org/10.1016/j.apenergy.2011.04.044>.
10. Preet S. Water and phase change material based photovoltaic thermal management systems: a review. *Renew Sustain Energy Rev*. 2018;82:791–807. <https://doi.org/10.1016/j.rser.2017.09.021>.
11. Yazdanifard F, Ameri M, Ebrahimi-Bajestan E. Performance of nanofluid-based photovoltaic/thermal systems: a review. *Renew Sustain Energy Rev*. 2017;76:323–52. <https://doi.org/10.1016/j.rser.2017.03.025>.
12. Aberoumand S, Ghamari S, Shabani B. Energy and exergy analysis of a photovoltaic thermal (PV/T) system using nanofluids: an experimental study. *Sol Energy*. 2018;165:167–77. <https://doi.org/10.1016/j.solener.2018.03.028>.
13. Al-Waeli AHA, Chaichan MT, Kazem HA, Sopian K. Comparative study to use nano-(Al₂O₃, CuO, and SiC) with water to enhance photovoltaic thermal PV/T collectors. *Energy Convers Manag*. 2017;148:963–73. <https://doi.org/10.1016/j.enconman.2017.06.072>.
14. Sardarabadi M, Hosseinzadeh M, Kazemian A, Passandideh-Fard M. Experimental investigation of the effects of using metal-oxides/water nanofluids on a photovoltaic thermal system (PVT) from energy and exergy viewpoints. *Energy*. 2017;138:682–95. <https://doi.org/10.1016/j.energy.2017.07.046>.
15. Said Z, Arora S, Bellos E. A review on performance and environmental effects of conventional and nanofluid-based thermal photovoltaics. *Renew Sustain Energy Rev*. 2018;94:302–16. <https://doi.org/10.1016/j.rser.2018.06.010>.
16. Fayaz H, Nasrin R, Rahim NA, Hasanuzzaman M. Energy and exergy analysis of the PVT system: effect of nanofluid flow rate. *Sol Energy*. 2018;169:217–30. <https://doi.org/10.1016/j.solener.2018.05.004>.
17. Nasrin R, Rahim NA, Fayaz H, Hasanuzzaman M. Water/MWCNT nanofluid based cooling system of PVT: experimental and numerical research. *Renew Energy*. 2018;121:286–300. <https://doi.org/10.1016/j.renene.2018.01.014>.
18. Abdallah SR, Saidani-Scott H, Abdellatif OE. Performance analysis for hybrid PV/T system using low concentration MWCNT (water-based) nanofluid. *Sol Energy*. 2019;181:108–15. <https://doi.org/10.1016/j.solener.2019.01.088>.
19. Alshaheen AA, Kianifar A, Rahimi AB. Experimental study of using nano-(GNP, MWCNT, and SWCNT)/water to investigate the performance of a PVT module. *J Therm Anal Calorim*. 2019. <https://doi.org/10.1007/s10973-019-08724-5>.
20. Arous S, Kayfeci M, Uysal A. Experimental investigations of using MWCNTs and graphene nanoplatelets water-based nanofluids as coolants in PVT systems. *Appl Therm Eng*. 2019;162:114265. <https://doi.org/10.1016/j.applthermaleng.2019.114265>.
21. Yazdanifard F, Ebrahimi-Bajestan E, Ameri M. Investigating the performance of a water-based photovoltaic/thermal (PV/T) collector in laminar and turbulent flow regime. *Renew Energy*. 2016;99:295–306. <https://doi.org/10.1016/j.renene.2016.07.004>.
22. Chow TT, Pei G, Fong KF, Lin Z, Chan ALS, Ji J. Energy and exergy analysis of photovoltaic–thermal collector with and without glass cover. *Appl Energy*. 2009;86(3):310–6. <https://doi.org/10.1016/j.apenergy.2008.04.016>.
23. Kazemian A, Hosseinzadeh M, Sardarabadi M, Passandideh-Fard M. Effect of glass cover and working fluid on the performance of photovoltaic thermal (PVT) system: an experimental study. *Sol Energy*. 2018;173:1002–10. <https://doi.org/10.1016/j.solener.2018.07.051>.
24. Said Z, Saidur R, Sabiha MA, Rahim NA, Anisur MR. Thermophysical properties of Single Wall Carbon Nanotubes and its effect on exergy efficiency of a flat plate solar collector. *Sol Energy*. 2015;115:757–69. <https://doi.org/10.1016/j.solener.2015.02.037>.
25. Haddad Z, Abid C, Mohamad AA, Rahli O, Bawazer S. Natural convection of silica–water nanofluids based on experimental measured thermophysical properties: critical analysis. *Heat Mass Transf*. 2016;52(8):1649–63. <https://doi.org/10.1007/s00231-015-1682-4>.
26. Drew DA, Passman SL. Theory of multicomponent fluids. Berlin: Springer; 2006.
27. Kazemian A, Hosseinzadeh M, Sardarabadi M, Passandideh-Fard M. Experimental study of using both ethylene glycol and phase change material as coolant in photovoltaic thermal systems (PVT) from energy, exergy and entropy generation viewpoints. *Energy*. 2018. <https://doi.org/10.1016/j.energy.2018.07.069>.
28. Hosseinzadeh M, Sardarabadi M, Passandideh-Fard M. Energy and exergy analysis of nanofluid based photovoltaic thermal system integrated with phase change material. *Energy*. 2018;147:636–47. <https://doi.org/10.1016/j.energy.2018.01.073>.

Publisher's Note Springer Nature remains neutral with regard to jurisdictional claims in published maps and institutional affiliations.